

# Fabrication and Characterization of Al<sub>2</sub>O<sub>3</sub> Based Electrical Insulation Coatings Around SiC Fibers

S. Palaniyappan, P. K. Chennam, M. Trautmann, H. Ahmad, T. Mehner, T. Lampke, G. Wagner

**Abstract**—In structural-health monitoring of fiber reinforced plastics (FRPs), every single inorganic fiber sensor that are integrated into the bulk material requires an electrical insulation around itself, when the surrounding reinforcing fibers are electrically conductive. This results in a more accurate data acquisition only from the sensor fiber without any electrical interventions. For this purpose, thin nano-films of aluminium oxide (Al<sub>2</sub>O<sub>3</sub>)-based electrical-insulation coatings have been fabricated around the Silicon Carbide (SiC) single fiber sensors through reactive DC magnetron sputtering technique. The sputtered coatings were amorphous in nature and the thickness of the coatings increased with an increase in the sputter time. Microstructural characterization of the coated fibers performed using scanning electron microscopy (SEM) confirmed a homogeneous circumferential coating with no detectable defects or cracks on the surface. X-ray diffraction (XRD) analyses of the as-sputtered and 2 hours annealed coatings (825 & 1125 °C) revealed the amorphous and crystalline phases of Al<sub>2</sub>O<sub>3</sub> respectively. Raman spectroscopic analyses produced no characteristic bands of Al<sub>2</sub>O<sub>3</sub>, as the thickness of the films was in the nanometer (nm) range, which is too small to overcome the actual penetration depth of the laser used. In addition, the influence of the insulation coatings on the mechanical properties of the SiC sensor fibers has been analyzed.

**Keywords**—Al<sub>2</sub>O<sub>3</sub> insulation coating, reactive sputtering, SiC single fiber sensor, single fiber tensile test.

## I. INTRODUCTION

FIBRE reinforced polymer matrix composites (PMCs) are replacing steel and other heavy materials in almost every applications like automobile, aerospace, sport, military etc., The main reason behind this replacement lies on their lightweight characteristics and the outstanding mechanical properties that they provide through reinforced structures. However, for an artefact free functionalization of these mechanical structures, an in-situ structural-health monitoring (SHM) of these complex structures becomes evident. Several sensors made up of carbon fibers, smart sensing filaments, smart sensing patches etc., [1], [2], [9] have already been developed to serve the mentioned purpose of SHM. But along with SHM, the sensors usually bring forth several artefacts together that alters the novel properties of the structures to a certain extent. Hence, the approach of using the fiber reinforcement itself as a sensor, with an aim to reduce or completely neglect these artefacts is essential. The process of data acquisition from the sensor fiber becomes difficult if the surrounding reinforcements are conductive in nature and

Saravanan Palaniyappan is with the Institute of Materials Science and Engineering, Chair of Composites and Material Compounds, Chemnitz University of Technology, 09125 Chemnitz, Germany (phone: +49 371 531-33873; fax: +49 371 531-833873; e-mail: saravanan.palaniyappan@mb.tu-chemnitz.de).

hence an electrical insulation around the fiber is very important. Al<sub>2</sub>O<sub>3</sub> thin films are often used in several applications [3], [4] because of their good adhesion to several substrates and highly recommended for applications of electrical-insulation coatings as they possess excellent dielectric properties and a wide band gap [5]. They are also thermally stable and resistant to oxidation at high temperatures [6]. Fabrication of thin film coatings around a single fiber has been researched for a variety of applications for a long time [8], [9]. Though there are several techniques such as physical vapor deposition (PVD), metal-organic chemical vapor deposition (MOCVD), atomic layer deposition (ALD) and sol-gel which are currently in use [4]-[7], the reactive sputtering process provides more opportunities to tailor the coating characteristics by varying different parameters of the process.

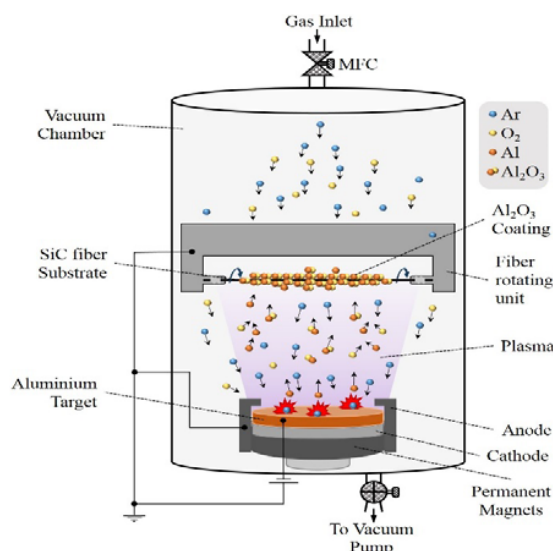


Fig. 1 Schematic of reactive sputtering of Al<sub>2</sub>O<sub>3</sub> around a single SiC fiber

In this part of the ongoing research, thin nano-films of Al<sub>2</sub>O<sub>3</sub> based electrical insulation coatings have been fabricated by reactive DC (Direct Current) magnetron sputtering around ceramic SiC fiber sensors and characterized.

## II. EXPERIMENTAL PROCEDURE

### A. Fabrication of the Coatings

For the fabrication of insulation coatings around the single SiC fibers (Tyranno SA3 fiber<sup>®</sup>, average diameter of 7.5 μm, UBE Industries Ltd.), a reactive DC magnetron sputtering

device has been used. An aluminium target (99.999% purity, Evochem GmbH) has been sputtered in vacuum with a base chamber pressure of around  $5 \times 10^{-5}$  mbar and a working pressure of  $8 \times 10^{-4}$  mbar. Argon (Ar, 99.9999% purity, Air Liquide Deutschland GmbH) and Oxygen ( $O_2$ , 99.9999% purity, Air Liquide Deutschland GmbH) have been used as sputtering and reactive gases respectively. The volume concentration of Ar and  $O_2$  has been maintained at a ratio of 3:1 controlled by a mass-flow controller (MFC). A DC magnetron sputtering power of 400 W has been applied to the target. Each single fiber has been coated for 60 min. The fibers (as bundles) are desized prior to the coating process in a tube furnace (Eurotherm, Ströhlein Instruments) at 500 °C for 2 h and a single fiber is mounted on a rotating unit that rotates at a constant speed of 3 rotations/min. The purpose of using such a rotation unit is to obtain a homogeneous coating around the circumference of the fiber. The target to substrate distance was set to be constant at 80 mm. A schematic representation of the fabrication process is shown in Fig. 1. For the XRD characterization, the same parameters are used to coat the insulation coating on flat silicon (Si) substrates with a coating time of 1 and 2 h accordingly. The Si substrates were treated in an ultrasonic bath containing acetone for 10 min before the deposition process and dried using nitrogen stream.

### B. Characterization of the Coatings

Raman spectroscopy characterizations (Renishaw inVia Raman spectrometer) were carried out using a Green laser (Nd: YAG) of wavelength 532 nm with 50 mW laser power. The samples were analyzed using 25 accumulations with 1 s each. For each set of samples, more than 5 different positions were analyzed using single-spot measurements. XRD phase analyses were carried out using a diffractometer (Bruker, D8 Discover) with  $Co-K_{\alpha}$  radiation. The XRD samples were analyzed by a point-focus beam using a 1 mm pinhole aperture and a LynxEye XE detector. The samples were tilted by  $5^\circ$  in order to avoid the single-crystal {400} peak of Si. The PDF-2014 data base (ICDD) was used for phase assignment. For the microstructural characterization, the coated and uncoated fibers were arranged on an aluminium sample holder with adhesive carbon tapes and SEM images (NEON 40EsB, Carl Zeiss) were taken. Mechanical characterization has been carried out using a Single fiber tensile testing module (Kammrath & Weiss) and always a single fiber of 10 mm length was taken and a linearly increasing tensile force with an elongation speed of  $2 \mu\text{m/s}$  was applied until break occurs.

## III. RESULTS AND DISCUSSION

### A. Phase Analyses (XRD & RAMAN)

For the characterization using XRD, the sputtered and annealed films on Si substrates were used instead of coated fibers as the dimensions of the single fiber were too small to examine the amorphous or crystalline nature of the coatings around them. The diffraction patterns of the sputtered and annealed thin films on Si substrate are shown in Fig. 2. It has been observed that the films deposited were amorphous in

nature and hence no peaks of  $Al_2O_3$  were observed on the sputtered films (both 1 h and 2 h deposition time).

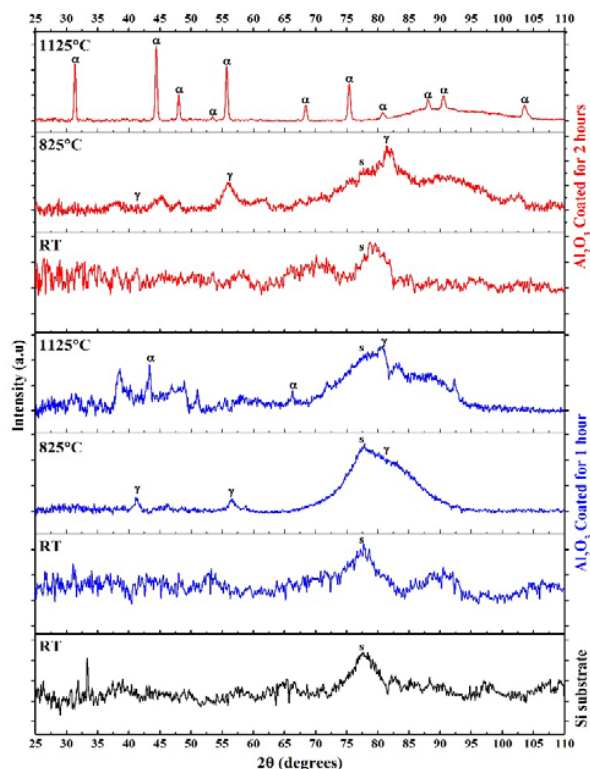


Fig. 2 XRD diffractograms of non-coated &  $Al_2O_3$  coated (1 h & 2 h) Si substrates at room temperature (RT) and after annealing at 825 °C or 1125 °C (s: Si substrate,  $\alpha$ :  $\alpha-Al_2O_3$ ,  $\gamma$ :  $\gamma-Al_2O_3$ )

The amorphous nature of the film could be attributed to the low fabrication temperature used, as the crystalline phases of  $Al_2O_3$  could only be obtained by maintaining a fabrication temperature greater than 700 °C [7]. However, after annealing in air at 825 °C for 2 h, some broad reflections of  $\gamma-Al_2O_3$  were observed, confirming the crystallization of the amorphous films. Similarly, after the samples were annealed at 1125 °C for 2 h, sharp reflections of  $\alpha-Al_2O_3$  were observed. This phase transformation from amorphous  $Al_2O_3$  to crystalline  $Al_2O_3$  agrees well with the previous literature [6], [7], [12], [14]. However, for the films deposited for 1 h, the reflections were not so intense due to the fact that the films were so thin ( $165 \pm 20$  nm) and it always had the background signals from the Si substrate.

Raman spectroscopic studies of the non-coated Si substrates, non-coated SiC fibers,  $Al_2O_3$ -coated Si and  $Al_2O_3$ -coated SiC fibers are shown in Fig. 3. In case of Si, the coated substrates have not produced any distinguishable bands other than Si band ( $519.8 \text{ cm}^{-1}$ ) due to the fact that the coatings are in the nm range, which is much lesser than the penetration depth of the laser source used. However, at some positions of analyses, a strong fluorescence background with a low intense graphitic band ( $1554 \text{ cm}^{-1}$ ) appeared. This could be due to the  $Al_2O_3$  coatings on the surface, which may have brought in

some impurities of carbon from the PVD reactor. Considering the SiC fibers, the sized and desized fibers have shown no distortion in the Raman bands confirming the temperature stability of SiC after the desizing process. It is also to be mentioned that the desizing parameter has been optimized in one of the previous works [13]. The Al<sub>2</sub>O<sub>3</sub>-coated fibers provided a different spectrum compared to the SiC fibers. A broad peak around 820 cm<sup>-1</sup> appeared with no additional bands of carbon. The usual transverse optical (TO) phonon band at 796 cm<sup>-1</sup> and longitudinal optical (LO) phonon band at 972 cm<sup>-1</sup> [16], which are characteristic of β-SiC fibers, disappeared. The peak at 820 cm<sup>-1</sup> could not be assigned to amorphous Al<sub>2</sub>O<sub>3</sub> as there are not sufficient literature references available so far to support the fact. The possible explanation could be that there occurs a shift of a peak towards higher or lower wavenumbers, whenever there is a compressive or tensile strain applied on any Raman active material respectively [17], [18]. This shift is caused by the incident photons gaining or losing energy from the lattice phonons resulting in a phenomenon called blue shift or red shift respectively [17], [18]. The TO mode which is supposed to be at 796 cm<sup>-1</sup> could have been shifted towards a higher wavenumber of around 820 cm<sup>-1</sup> due to the compressive strain delivered by the Al<sub>2</sub>O<sub>3</sub> coating on the fiber lattice. Another possibility could be that if there has been an introduction of structural disorders in the SiC lattice due to the Al<sub>2</sub>O<sub>3</sub> coating, a symmetrical broadening of TO mode is expected to occur [15]. Hence in this case, it could be explained in such a way that a broader TO band is seen in Fig. 3 with a blue shift of approximately 24 cm<sup>-1</sup>. However, a deeper investigation of these justification principles is still ongoing.

### B. Mechanical Characterization

The mechanical testing characteristics of sized (received from manufacturer), desized (in air at 500 °C for 2 hours) and Al<sub>2</sub>O<sub>3</sub>-coated fibers is plotted in Fig. 4.

It has been observed that the tensile strength of the sized fiber gets degraded by approximately 11 % after the process of thermal desizing. This degradation could be attributed to abnormal SiC crystal growth or surface flaws caused by pore formation on the surface of the fibers [10], [11]. From the previous work [13], it has been identified that the desizing at 500 °C for 2 hours provided an increased roughness to the fibers. It has been considered as an advantageous remark for the further coating process of fibers using PVD, as a rougher surface is expected to provide a better adhesion to the incoming coating materials than a smoother surface. Analyzing the mechanical characterization results of Al<sub>2</sub>O<sub>3</sub> coated fibers, it has been seen that the mechanical property is almost being restored to its original state after the fibers are coated with Al<sub>2</sub>O<sub>3</sub>. But however, there is still a tensile strength degradation of around 2 % in the coated fibers as compared to the tensile strength of sized fibers.

The possible explanation for this restoration could be that the very thin film of Al<sub>2</sub>O<sub>3</sub>-coating on the fiber surface could have healed up the surface flaws to some extent and helped the coated fibers in retaining the tensile stress a little longer than

the desized ones. Even though an approximate 23 % reduction of the breaking elongation is observed in the coated fibers compared to the sized ones, a lower standard deviation confirms the fact that the surface flaws could have been healed up by the coating material. In addition, the Young's Modulus (E-Modulus) of the coated and non-coated fibers was found to be 620 ± 90 GPa and 430 ± 50 GPa respectively. The E-Modulus increased by a factor of 0.4 in the Al<sub>2</sub>O<sub>3</sub>-coated fibers as compared to the non-coated sized ones.

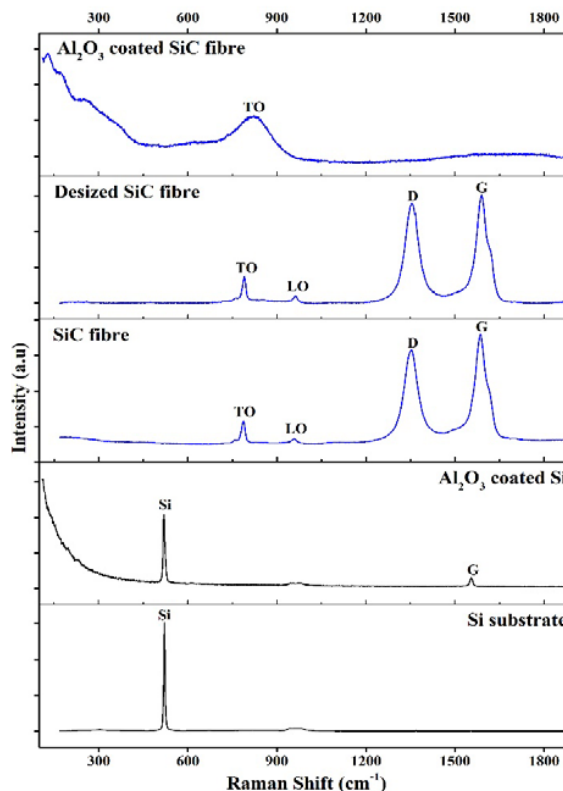


Fig. 3 Raman spectroscopic analyses of non-coated Si and Al<sub>2</sub>O<sub>3</sub>-coated Si for 1 h (black); non-coated SiC fiber, desized SiC fiber and Al<sub>2</sub>O<sub>3</sub>-coated SiC fiber for 1 h (blue); Si: Si band; D, G: carbon bands; TO, LO: SiC bands

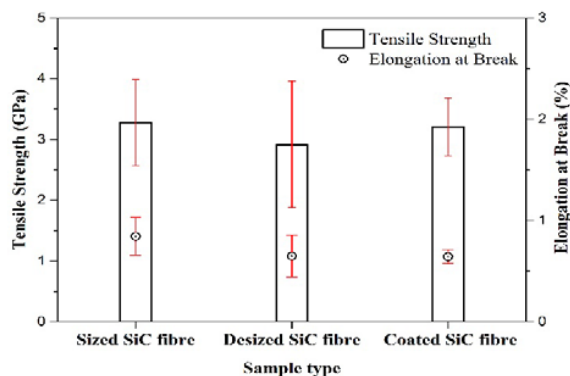


Fig. 4 Single fiber tensile test analyses performed on sized, desized and Al<sub>2</sub>O<sub>3</sub> coated SiC single fibers (average of 10 experimental results each)

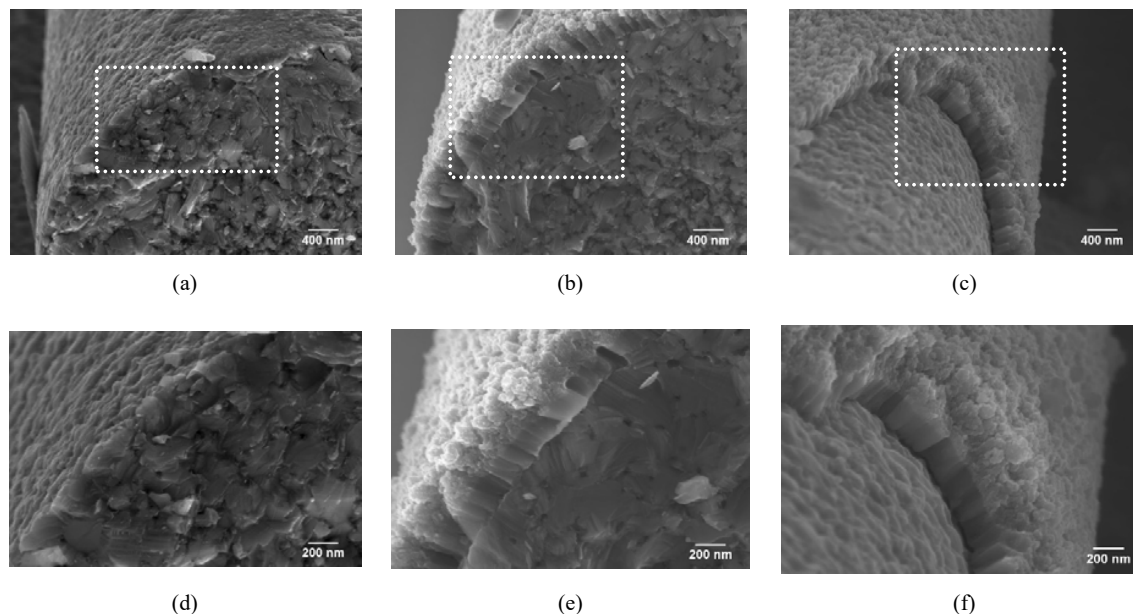


Fig. 5 SEM micrographs of non-coated and  $\text{Al}_2\text{O}_3$ -coated SiC single fibers: (a) Non-coated sized fiber; (b) Cross-sectional view and (c) side view of the fracture surface of  $\text{Al}_2\text{O}_3$ -coated SiC fiber; (d), (e), (f) 2x magnification of inset marked area

### C. Microstructural Characterization

The microstructural investigations performed on the non-coated and  $\text{Al}_2\text{O}_3$ -coated fibers using SEM are shown in Fig. 5. The  $\text{Al}_2\text{O}_3$  thin film is homogeneous around the circumference of the fiber with good adhesion to the underlying fiber substrate. The coatings are found to be  $(165 \pm 20)$  nm thick and the thickness seemed to be varying slightly in the range of a few nm along the longitudinal axis of the fiber. This varying thickness could be due to the outer race track poisoning effect of the sputtering target caused by the deposition of  $\text{Al}_2\text{O}_3$  onto the Al target and the sputtering chamber itself. This results in the accumulation of electric charges from the plasma and leads to an uneven removal of sputtering atom from the target surface. This effect could be reduced further by using a pulsed DC magnetron sputtering technique [19]. The  $\text{Al}_2\text{O}_3$  coatings are found to be free from cracks or other defects and the thin film with a columnar, porous, cauliflower shaped surface features correlate with the nucleation and growth theories (Zone 1 with  $T_s < 0.3 T_m$ ) proposed so far [20].

### IV. SUMMARY AND CONCLUSION

Fabrication of  $\text{Al}_2\text{O}_3$ -based electrical-insulation coatings around SiC fiber sensors have been accomplished using reactive DC magnetron sputtering technique. The as-sputtered amorphous  $\text{Al}_2\text{O}_3$  coatings are capable of crystallizing into  $\gamma$ - $\text{Al}_2\text{O}_3$  and  $\alpha$ - $\text{Al}_2\text{O}_3$  phases after being annealed for 2 h in air at 825 °C and 1125 °C respectively. The coatings are found to be homogeneous around the circumference of the fibers with very few or negligible number of voids and defects in the interface. Due to a nm thick coating, the effects of residual stress is negligible and further the surface defects or flaws caused by desizing temperature have been healed by the thin

$\text{Al}_2\text{O}_3$  coating. This is very well revealed by the increasing tensile strength of the coated fibers in comparison to the desized fibers. Hence the fabrication of a tailor-made  $\text{Al}_2\text{O}_3$  based electrical-insulation coating in the nm range is feasible with the reactive DC magnetron sputtering technique.

### ACKNOWLEDGMENT

The corresponding author S. Palaniyappan would like to thank the financial support of the 'Sächsische Aufbaubank (SAB)' in the framework of 'ESF Landesinnovations-promotionen' and the laboratory support of the Chair of Composites and Material Compounds, Institute of Materials Science and Engineering, Chemnitz University of Technology towards this research work.



### REFERENCES

- [1] S. Nauman, Z. Asfar, I. Cristian, C. Loghin, and V. Koncar, "14 - Smart textiles for structural health monitoring of composite structures," in *Smart Textiles and their Applications*, V. Koncar, Ed. Oxford: Woodhead Publishing, 2016, pp. 309–328.
- [2] C. Cherif, E. Haentzsch, R. Mueller, A. Nocke, M. Huebner, and M. M. B. Hasan, "15 - Carbon fiber sensors embedded in glass fiber-based composites for windmill blades," in *Smart Textiles and their Applications*, V. Koncar, Ed. Oxford: Woodhead Publishing, 2016, pp. 329–352.
- [3] Landolt-Bornstein, New Series, Group IV, Vol. 5.a, Vol. 7, Springer, Berlin.
- [4] J. M. Schneider, W.D. Sproul, A. Matthews, "Reactive Ionized Magnetron Sputtering of Crystalline Alumina coatings", *Surf. Coat. Technol.* 98, 1473- 1476, 1998.
- [5] S. Dutta, S. Ramesh, B. Shankar, and S. Gopalan, "Effect of PVD process parameters on the quality and reliability of thin (10–30 nm)  $\text{Al}_2\text{O}_3$  dielectrics," *Applied Nanoscience*, vol. 2, no. 1, pp. 1–6, Mar. 2012.

- [6] L. Zhang, H. C. Jiang, C. Liu, J. W. Dong, and P. Chow, "Annealing of Al<sub>2</sub>O<sub>3</sub> thin films prepared by atomic layer deposition," *Journal of Physics D: Applied Physics*, vol. 40, no. 12, pp. 3707–3713, Jun. 2007.
- [7] J. C. Nable, M. K. Gulbinska, M. A. Kmetz, S. L. Suib, and F. S. Galasso, "Aluminum Oxide and Chromium Oxide Coatings on Ceramic Fibers via MOCVD," *Chemistry of Materials*, vol. 15, no. 25, pp. 4823–4829, Dec. 2003.
- [8] K. Roder et al., "Development of a SiN<sub>x</sub>-Based Barrier Coating for SiC Fibers," *Materials Science Forum*, vol. 825–826, pp. 256–263, Jul. 2015.
- [9] T. Mäder, D. Nestler, and B. Wielage, "Strain sensing using single carbon fibers," p. 7.
- [10] H. Oda and T. Ishikawa, "Microstructure and mechanical properties of SiC-polycrystalline fiber and new defect-controlling process," *International Journal of Applied Ceramic Technology*, vol. 14, no. 6, pp. 1031–1040, Nov. 2017.
- [11] S. Cao, J. Wang, and H. Wang, "Formation mechanism of large SiC grains on SiC fiber surfaces during heat treatment," *CrystEngComm*, vol. 18, no. 20, pp. 3674–3682, 2016.
- [12] S. Blittersdorf, N. Bahlawane, K. Kohse-Höinghaus, B. Atakan, and J. Müller, "CVD of Al<sub>2</sub>O<sub>3</sub> Thin Films Using Aluminum Triisopropoxide," *Chem. Vap. Depos.*, vol. 9, no. 4, pp. 194–198, 2003.
- [13] S. Palaniyappan, T. Ega, G. Wagner, "Influence of nano Roughness on the Electrical resistance of SiC micro fibers", Poster Contribution, 20. Werkstofftechnischen Kolloquium (WTK 2018), 14-15. March 2018, Chemnitz, Germany.
- [14] A. E. Muhsin, Dissertation, "Chemical Vapor Deposition of Aluminium Oxide (Al<sub>2</sub>O<sub>3</sub>) and Beta Iron Disilicide (β-FeSi<sub>2</sub>) Thin Films," 2007.
- [15] S. Nakashima and H. Harima, "Raman Investigation of SiC Polytypes," *physica status solidi (a)*, vol. 162, no. 1, pp. 39–64, Jul. 1997.
- [16] J. Wasyluk, T. S. Perova, S. A. Kukushkin, A. V. Osipov, N. A. Feoktistov, and S. A. Grudinkin, "Raman Investigation of Different Polytypes in SiC Thin Films Grown by Solid-Gas Phase Epitaxy on Si (111) and 6H-SiC Substrates," *Materials Science Forum*, vol. 645–648, pp. 359–362, Apr. 2010.
- [17] K. N. Kudin, B. Ozbas, H. C. Schniepp, R. K. Prud'homme, I. A. Aksay, and R. Car, "Raman Spectra of Graphite Oxide and Functionalized Graphene Sheets," *Nano Letters*, vol. 8, no. 1, pp. 36–41, Jan. 2008.
- [18] C. Y. Xu, P. X. Zhang, and L. Yan, "Blue shift of Raman peak from coated TiO<sub>2</sub> nanoparticles," *Journal of Raman Spectroscopy*, vol. 32, no. 10, pp. 862–865, Oct. 2001.
- [19] A. Belkind, A. Freilich, J. Lopez, Z. Zhao, W. Zhu, and K. Becker, "Characterization of pulsed dc magnetron sputtering plasmas," *New J. Phys.*, vol. 7, pp. 90–90, Apr. 2005.
- [20] B. A. Movchan, A. V. Demchishin - *Fizika Metallov Metallovedenie, Structure and Properties of thick condensates Of Nickel, Titanium, Tungsten, Aluminum oxides, And Zirconium dioxide In Vacuum* 1969.